

Back-to-back relative-excess observable in search for the chiral magnetic effect

Yicheng Feng,^{1,*} Jie Zhao,^{1,†} and Fuqiang Wang^{1,2,‡}

¹*Department of Physics and Astronomy, Purdue University, West Lafayette, IN 47907, USA*

²*School of Science, Huzhou University, Huzhou, Zhejiang 313000, China*

(Dated: February 11, 2021)

Background: The chiral magnetic effect (CME) is extensively studied in heavy-ion collisions at RHIC and LHC. In the commonly used reaction plane (RP) dependent, charge dependent azimuthal correlator ($\Delta\gamma$), both the close and back-to-back pairs are included. Many backgrounds contribute to the close pairs (e.g. resonance decays, jet correlations), whereas the back-to-back pairs are relatively free of those backgrounds.

Purpose: In order to reduce those backgrounds, we propose a new observable which only focuses on the back-to-back pairs, namely, the relative back-to-back opposite-sign (OS) over same-sign (SS) pair excess (r_{BB}) as a function of the pair azimuthal orientation with respect to the RP (φ_{BB}).

Methods: We use analytical calculations and toy model simulations to demonstrate the sensitivity of $r_{\text{BB}}(\varphi_{\text{BB}})$ to the CME and its insensitivity to backgrounds.

Results: With finite CME, the φ_{BB} distribution of r_{BB} shows a clear characteristic modulation. Its sensitivity to background is significantly reduced compared to the previous $\Delta\gamma$ observable. The simulation results are consistent with our analytical calculations.

Conclusions: Our studies demonstrate that the $r_{\text{BB}}(\varphi_{\text{BB}})$ observable is sensitive to the CME signal and rather insensitive to the resonance backgrounds.

PACS numbers: 25.75.-q, 25.75.-Gz, 25.75.-Ld

1. INTRODUCTION

In quantum chromodynamics (QCD), vacuum fluctuations can produce nontrivial topological gluon fields in local domains [1]. The chirality of quarks, under the approximate chiral symmetry, is imbalanced in those gluon fields [2–4]. This violates the \mathcal{CP} symmetry in QCD in local domains. In a strong magnetic field, the single-handed quarks will polarize along or opposite to the magnetic field depending on the quark charge. This produces an electric current along the magnetic field, resulting in an observable charge separation in the final state [3, 4]. This phenomenon is called the chiral magnetic effect (CME) [3, 4].

In non-central heavy-ion collisions, the spectator protons can produce an intense, transient magnetic field, approximately perpendicular to the reaction plane (RP) (spanned by the beam direction and the impact parameter) [4]. The high energy density region created in these collisions, where the approximate chiral symmetry may be restored, provides a suitable environment to search for the CME [4]. The observation of CME-induced charge separation in heavy-ion collisions would provide a strong evidence for QCD vacuum fluctuations and local \mathcal{CP} violation.

The CME is extensively studied in heavy-ion experiments at the Relativistic Heavy Ion Collider (RHIC) [5–12] and the Large Hadron Collider (LHC) [13–16].

To probe the CME signal, the RP-dependent, charge-dependent $\Delta\gamma$ observable was proposed [17] and widely used. Positive CME-like signals in $\Delta\gamma$ have been observed in both heavy ion collisions (Au+Au at RHIC [5–8] and Pb+Pb at the LHC [14]) and small systems collisions (p+Au and d+Au at RHIC [9, 10] and p+Pb at the LHC [13]), where the latter is believed to come only from backgrounds. In fact, it has been pointed out previously that the $\Delta\gamma$ in heavy-ion collisions was contaminated by major backgrounds [18–20]. Various methods have been developed to suppress the backgrounds, such as event shape engineering [15, 16], invariant mass dependence [9], and the comparative $\Delta\gamma$ measurements with respect to the reaction and participant planes [21, 22]. The current results with those methods show a CME signal consistent with zero.

In this paper, we propose a new method. In the original definition of $\Delta\gamma$, both the close pairs and the back-to-back pairs are included. Many backgrounds contribute to the close pairs (e.g. resonance decays, jet correlations) [18–20, 23–30], whereas the back-to-back pairs are relatively free of those backgrounds. Thus, we propose a new observable which only focuses on the back-to-back pairs, namely, the relative back-to-back opposite-sign (OS) over same-sign (SS) pair excess as a function of the pair azimuthal orientation with respect to the RP. We use simulations by a toy model (previously used in Ref. [31, 32]) to demonstrate the sensitivity of this observable to the CME signal and insensitivity to the backgrounds. The relationship between this new observable and the $\Delta\gamma$ observable is also discussed.

The paper is organized as follows. Section 2 describes the methodology of this study. Section 3 shows our toy-model simulation results using the new method. Sec-

* feng216@purdue.edu

† zhao656@purdue.edu

‡ fqwang@purdue.edu

$$\begin{aligned}
n_{SS}(\varphi_{BB}) &= \int_{\delta=-\Delta}^{\delta=\Delta} n_{SS}(\varphi_{BB}, \delta) d\delta \\
&= \frac{2\langle N^2 \rangle}{\pi^2} \left[\Delta + (v_{2,\pi^+}^2 + v_{2,\pi^-}^2) \Delta \cos 4\varphi_{BB} - a_1^2 \sin 2\Delta \right. \\
&\quad \left. + \cos 2\varphi_{BB} (2a_1^2 \Delta + (v_{2,\pi^+} + v_{2,\pi^-}) \sin 2\Delta) \right. \\
&\quad \left. + \frac{1}{4} (v_{2,\pi^+}^2 + v_{2,\pi^-}^2) \sin 4\Delta \right].
\end{aligned} \tag{9}$$

The difference and sum are, respectively,

$$\begin{aligned}
n_{OS}(\varphi_{BB}) - n_{SS}(\varphi_{BB}) &= \frac{2\langle N^2 \rangle}{\pi^2} \left[-4a_1^2 \Delta \cos 2\varphi_{BB} + 2a_1^2 \sin 2\Delta \right. \\
&\quad \left. - (v_{2,\pi^+} - v_{2,\pi^-})^2 \Delta \cos 4\varphi_{BB} \right. \\
&\quad \left. - \frac{1}{4} (v_{2,\pi^+} - v_{2,\pi^-})^2 \sin 4\Delta \right],
\end{aligned} \tag{10}$$

$$\begin{aligned}
n_{OS}(\varphi_{BB}) + n_{SS}(\varphi_{BB}) &= \frac{2\langle N^2 \rangle}{\pi^2} \left[2\Delta + (v_{2,\pi^+} + v_{2,\pi^-})^2 \Delta \cos 4\varphi_{BB} \right. \\
&\quad \left. + (v_{2,\pi^+} + v_{2,\pi^-}) \cos 2\varphi_{BB} \sin 2\Delta \right. \\
&\quad \left. + \frac{1}{4} (v_{2,\pi^+} + v_{2,\pi^-})^2 \sin 4\Delta \right].
\end{aligned} \tag{11}$$

Our new observable is the ratio and we expand it into Fourier series

$$r_{BB}(\varphi_{BB}) = \frac{n_{OS}(\varphi_{BB}) - n_{SS}(\varphi_{BB})}{n_{OS}(\varphi_{BB}) + n_{SS}(\varphi_{BB})} = \sum_{k=0}^{+\infty} c_k \cos(k\varphi_{BB}). \tag{12}$$

Noticing that $(v_{2,\pi^+} + v_{2,\pi^-})$ is small (~ 0.1), up to the first order of $(v_{2,\pi^+} + v_{2,\pi^-})$, the coefficient of $\cos 2\varphi_{BB}$ is

$$\begin{aligned}
c_2 \approx a_1^2 \left(-2 - (v_{2,\pi^+} + v_{2,\pi^-}) \frac{\sin^2 2\Delta}{\Delta^2} \right) \\
+ (v_{2,\pi^+} + v_{2,\pi^-})(v_{2,\pi^+} - v_{2,\pi^-})^2 \frac{(2\Delta + \sin 4\Delta) \sin 2\Delta}{8\Delta^2}.
\end{aligned} \tag{13}$$

If we require the opening angle to be larger than 150° for the back-to-back pairs, then $\Delta = 15^\circ$,

$$\begin{aligned}
c_2 \approx a_1^2 (-2 - 3.648(v_{2,\pi^+} + v_{2,\pi^-})) \\
+ 1.267(v_{2,\pi^+} + v_{2,\pi^-})(v_{2,\pi^+} - v_{2,\pi^-})^2.
\end{aligned} \tag{14}$$

The second term is not related to the CME; taking $|v_{2,\pi^+} - v_{2,\pi^-}| \sim 10^{-3}$, $(v_{2,\pi^+} + v_{2,\pi^-}) \sim 10^{-1}$, its magnitude is on the order of 10^{-7} . For a CME signal of $a_1 \geq 10^{-3}$, a_1^2 dominates over the primordial flow effects in c_2 , indicating that c_2 is a good measure of the CME.

Similarly, the coefficient of the constant term ($k = 0$) is

$$\begin{aligned}
c_0 = \frac{\sin 2\Delta}{4\Delta} (4a_1^2(1 + v_{2,\pi^+} + v_{2,\pi^-}) \\
- (v_{2,\pi^+} - v_{2,\pi^-})^2 \cos 2\Delta),
\end{aligned} \tag{15}$$

and for $\Delta = 15^\circ$,

$$c_0 \approx 1.910a_1^2(1 + v_{2,\pi^+} + v_{2,\pi^-}) - 1.654(v_{2,\pi^+} - v_{2,\pi^-})^2. \tag{16}$$

Note that c_2 and c_0 are both sensitive to the CME, with similar sensitivities. It will be shown later, however, that c_0 is also sensitive to the backgrounds. Those backgrounds are mainly from the low p_T resonance decays whose decay daughters are back-to-back. The c_2 is less sensitive to those backgrounds because their v_2 at low p_T is small.

2.3. Comparison to the back-to-back $\Delta\gamma$ observable, $\Delta\gamma_{BB}$

The $\Delta\gamma$ observable is frequently used in heavy-ion collisions to search for the CME,

$$\begin{aligned}
\Delta\gamma &= \gamma_{OS} - \gamma_{SS}, \\
\gamma &= \langle \cos(\varphi_1 + \varphi_2) \rangle.
\end{aligned} \tag{17}$$

To see the relationship between r_{BB} and $\Delta\gamma$, we will apply the same ‘‘back-to-back’’ requirement to the pairs in $\Delta\gamma$, denoted as $\Delta\gamma_{BB}$. For back-to-back pairs, $\cos(\varphi_1 + \varphi_2) = -\cos(2\varphi_{BB})$. The correlators γ_{OS} and γ_{SS} can be simplified into

$$\begin{aligned}
\gamma_{OS} &= - \frac{\int \cos(2\varphi_{BB}) n_{OS}(\varphi_{BB}) d\varphi_{BB}}{\int n_{OS}(\varphi_{BB}) d\varphi_{BB}} \\
&= \frac{2a_1^2 \Delta - (v_{2,\pi^+} + v_{2,\pi^-}) \sin 2\Delta}{2\Delta + 2a_1^2 \sin 2\Delta + v_{2,\pi^-} v_{2,\pi^+} \sin 4\Delta}, \\
\gamma_{SS} &= - \frac{\int \cos(2\varphi_{BB}) n_{SS}(\varphi_{BB}) d\varphi_{BB}}{\int n_{SS}(\varphi_{BB}) d\varphi_{BB}} \\
&= \frac{-2a_1^2 \Delta - (v_{2,\pi^+} + v_{2,\pi^-}) \sin 2\Delta}{2\Delta - 2a_1^2 \sin 2\Delta + \frac{1}{2}(v_{2,\pi^-}^2 + v_{2,\pi^+}^2) \sin 4\Delta}.
\end{aligned} \tag{18}$$

The difference to the first order of $(v_{2,\pi^+} + v_{2,\pi^-})$ is therefore

$$\begin{aligned}
\Delta\gamma_{BB} &= \gamma_{OS} - \gamma_{SS} \\
&\approx a_1^2 \left(2 + (v_{2,\pi^+} + v_{2,\pi^-}) \frac{\sin^2 2\Delta}{\Delta^2} \right) \\
&\quad - (v_{2,\pi^+} + v_{2,\pi^-})(v_{2,\pi^+} - v_{2,\pi^-})^2 \frac{\sin 2\Delta \sin 4\Delta}{8\Delta^2}.
\end{aligned} \tag{19}$$

With $\Delta = 15^\circ$, it becomes

$$\begin{aligned}
\Delta\gamma_{BB} &= \gamma_{OS} - \gamma_{SS} \\
&\approx a_1^2 (2 + 3.648(v_{2,\pi^+} + v_{2,\pi^-})) \\
&\quad - 0.790(v_{2,\pi^+} + v_{2,\pi^-})(v_{2,\pi^+} - v_{2,\pi^-})^2.
\end{aligned} \tag{20}$$

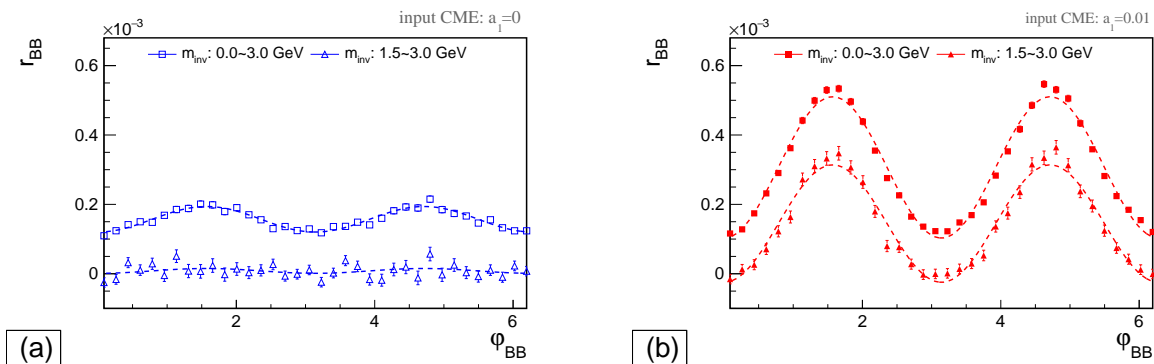


FIG. 2. The distribution of the back-to-back relative-excess observable $r_{\text{BB}}(\varphi_{\text{BB}})$ in the toy model simulations with input CME (a) $a_1 = 0$ and (b) $a_1 = 0.01$.

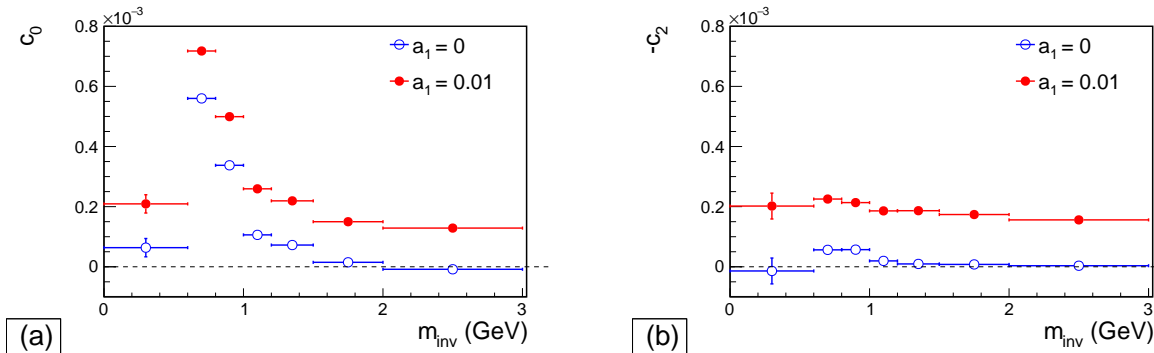


FIG. 3. The fitted Fourier coefficients, (a) c_0 and (b) $-c_2$, to the back-to-back relative-excess observable $r_{\text{BB}}(\varphi_{\text{BB}})$ in the toy model with various CME inputs.

Comparing Eqs. 19 and 20 to Eqs. 13 and 14, it is clear that $\Delta\gamma_{\text{BB}}$ and r_{BB} have similar sensitivity to the CME. The r_{BB} observable is directly related to $\Delta\gamma_{\text{BB}}$. Only the back-to-back pairs are used in these two observables, so the backgrounds among the close pairs are reduced.

3. RESULTS

In this section, we show the back-to-back $r_{\text{BB}}(\varphi_{\text{BB}})$ and back-to-back $\Delta\gamma_{\text{BB}}$ observables calculated from a toy model (with/without input CME) simulations.

3.1. Toy-model simulation

We use a toy model including the primordial pions and the ρ meson decays to study the sensitivities of r_{BB} to CME signal and resonance backgrounds. This toy model has been used for CME background studies in Ref. [31, 32]. Both the resonance decays and primordial pions have the p_T distributions and $v_2(p_T)$ obtained from Au+Au measurements corresponding to centrality 40% \sim 50% [31, 33–42].

To simulate the CME signal in the toy model, we input the coefficient a_1 when generating the primordial pi-

ons from the azimuthal distribution (Eq. 3). Two cases are studied, one without CME input ($a_1 = 0$), and the other with 1% CME input ($a_1 = 0.01$). Each case has 2×10^9 events. The tracks are selected with transverse momentum $0.2 \text{ GeV} < p_T < 2.0 \text{ GeV}$ and pseudorapidity $-1.0 < \eta < 1.0$. Figure 2 shows the $r_{\text{BB}}(\varphi_{\text{BB}})$ distributions for the two cases. The case with finite CME shows larger amplitude and modulation than the case without, indicating the sensitivity of the $r_{\text{BB}}(\varphi_{\text{BB}})$ observable to the CME. The case without CME shows some finite amplitude and modulation, at low m_{inv} , indicating that the observable still has some background contamination. In order to further suppress resonance backgrounds, we also show the r_{BB} distributions with the invariant mass range $1.5 \text{ GeV} < m_{\text{inv}} < 3.0 \text{ GeV}$. The result is consistent with zero as expected.

We fit the $r_{\text{BB}}(\varphi_{\text{BB}})$ distributions to Eq. 12. Figure 3 shows the fitted Fourier coefficients c_0 and $-c_2$, respectively, as a function of m_{inv} . The c_0 has strong sensitivity to both signal and background. Although still affected by the residual resonance backgrounds, the $-c_2$ has better sensitivity to CME than c_0 and less sensitivity to background. To illustrate our results more quantitatively, we list the fitted coefficients c_0 and $-c_2$ in Table I. Also listed are the a_1 values extracted from c_0 and $-c_2$, via Eqs. 16 and 14, respectively, ignoring the presence of

m_{inv} range (GeV)	input a_1	Fourier coefficients ($\times 10^{-4}$)		extracted a_1 ($\times 10^{-2}$)
0.0 \sim 3.0	0	c_0	1.57 ± 0.01	0.87 ± 0.01
		$-c_2$	0.37 ± 0.02	0.39 ± 0.02
	0.01	c_0	3.07 ± 0.01	1.21 ± 0.01
		$-c_2$	2.04 ± 0.02	0.93 ± 0.01
1.5 \sim 3.0	0	c_0	0.08 ± 0.03	0.20 ± 0.07
		$-c_2$	0.07 ± 0.04	0.17 ± 0.10
	0.01	c_0	1.45 ± 0.03	0.83 ± 0.02
		$-c_2$	1.69 ± 0.04	0.85 ± 0.02

TABLE I. The fitted Fourier coefficients c_0 and $-c_2$ are shown for the $r_{\text{BB}}(\varphi_{\text{BB}})$ distributions from the toy-model simulations with/without CME signal input. Two invariant mass ranges are shown. If we set $(v_{2,\pi^+} + v_{2,\pi^-}) \approx 0.1$, ignore the $(v_{2,\pi^+} - v_{2,\pi^-})^2$ terms in Eqs. 14 and 16, and assume zero resonance background in the toy-model simulations, the a_1 can be extracted from c_0 and c_2 , respectively. These extracted a_1 values are also listed, to be compared to the input a_1 .

backgrounds. Due to resonance backgrounds in the low m_{inv} range, the extracted a_1 are large with $0.0 \text{ GeV} < m_{\text{inv}} < 3.0 \text{ GeV}$, no matter whether the input a_1 are zero or not. In the range $1.5 \text{ GeV} < m_{\text{inv}} < 3.0 \text{ GeV}$, with zero input a_1 , the extracted a_1 values are also close to zero; the small deviations from zero are due to residual resonance backgrounds. With input $a_1 = 0.01$, the extracted a_1 values in the high m_{inv} range are nonzero, close to the input; again, the differences are due to residual resonance backgrounds. However, under this condition, the extracted a_1 values are smaller than the inputs. This is because there are pairs composed of pions from uncorrelated sources (one primordial pion and one resonance pion, or two pions from two different resonance decays), whose zero contributions are averaged in c_0 , $-c_2$. The dilution from those uncorrelated pairs reduces the extracted a_1 values.

3.2. Comparison among $\Delta\gamma$, $\Delta\gamma_{\text{BB}}$, and $-c_2$

We also calculate the inclusive $\Delta\gamma$ and back-to-back $\Delta\gamma_{\text{BB}}$ observables in our model studies. Figure 4 compares the results of those three observables. It is found that $\Delta\gamma_{\text{BB}}$ and $-c_2$ are very close to each other. This indicates that the r_{BB} and $\Delta\gamma_{\text{BB}}$ observables are nearly the same, as expected from Eqs. 14 and 20. With zero CME input ($a_1 = 0$) in the toy model simulation (Fig. 4a), the inclusive $\Delta\gamma$ is further away from zero than the other two observables in the invariant mass range $0.6 \sim 1.5 \text{ GeV}$ where resonance contributions are large. This shows that the inclusive $\Delta\gamma$ is more significantly affected by the resonance backgrounds. In the high mass region where resonance contributions are small, all three observables approach to zero as expected. With nonzero CME input ($a_1 = 0.01$) in the toy model simulation (Fig. 4b), the three observables are all away from zero. The inclusive $\Delta\gamma$ is lower than the other two in the mass range $1.5 \text{ GeV} \sim 3.0 \text{ GeV}$ where there is not much resonance contribution. This is because the back-to-back CME signal is diluted more in the inclusive $\Delta\gamma$ by including close

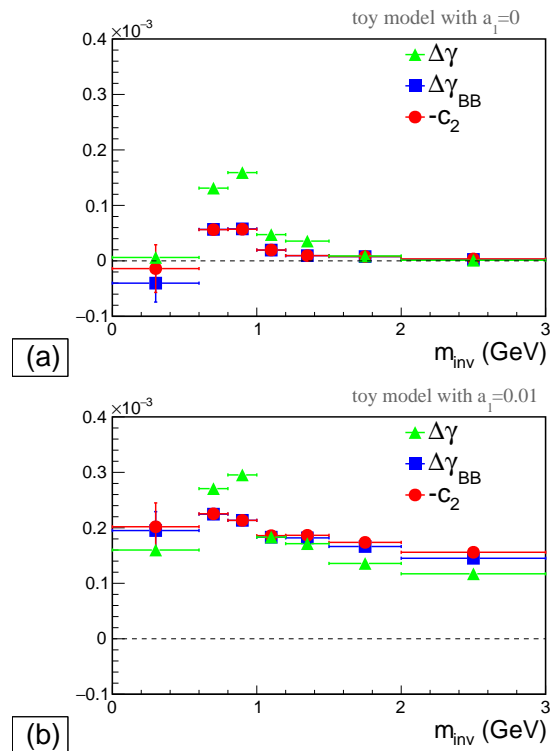


FIG. 4. Comparison among the inclusive $\Delta\gamma$, the back-to-back $\Delta\gamma_{\text{BB}}$, and the Fourier coefficient $-c_2$ of the $r_{\text{BB}}(\varphi_{\text{BB}})$ distribution in different simulations.

pairs from backgrounds. This can also be explained by the analytical calculations in Eq. 19 by assigning $\Delta = 90^\circ$ for the inclusive $\Delta\gamma$ and $\Delta = 15^\circ$ for $\Delta\gamma_{\text{BB}}$.

4. SUMMARY

In this paper, we propose a new observable to search for the CME, called the back-to-back relative-excess observable of OS to SS pairs (r_{BB}), as a function of the pair azimuthal orientation (φ_{BB}). The charge pairs used

in this observable are required to be back-to-back: opening angle larger than 150° on the transverse plane; they are taken from different η ranges with a $\Delta\eta$ gap to further reduce backgrounds. As a result, the backgrounds (such as resonance decays) contributing mostly to the close pairs can be reduced. A modulation of the form $\cos 2\varphi_{\text{BB}}$ in the observable can indicate a CME signal, which is described by the second-order coefficient c_2 in Fourier expansion.

We use a toy model simulation without input CME ($a_1 = 0$) and with 1% input CME ($a = 0.01$), and calculate the observable from the simulated data. The coefficient c_2 is close to zero when there is no input CME, whereas it is far from zero with 1% input CME.

To relate the new observable to the previous $\Delta\gamma$ ob-

servable, we apply the same back-to-back pair requirement to the definition of $\Delta\gamma$ to obtain $\Delta\gamma_{\text{BB}}$. We use analytical calculations and toy-model simulations to show that $\Delta\gamma_{\text{BB}}$ is nearly identical to $-c_2$. Both are more sensitive to the CME and less sensitive to resonance backgrounds than the inclusive $\Delta\gamma$ observable.

ACKNOWLEDGMENTS

This work is supported in part by the U.S. Department of Energy Grant No. DE-SC0012910 and the National Natural Science Foundation of China Grant No. 11847315.

-
- [1] T. Lee and G. Wick, Vacuum stability and vacuum excitation in a spin 0 field theory, *Phys.Rev.* **D9**, 2291 (1974).
- [2] P. D. Morley and I. A. Schmidt, Strong P, CP, T violations in heavy ion collisions, *Z. Phys.* **C26**, 627 (1985).
- [3] D. Kharzeev, R. Pisarski, and M. H. Tytgat, Possibility of spontaneous parity violation in hot QCD, *Phys.Rev.Lett.* **81**, 512 (1998), arXiv:hep-ph/9804221 [hep-ph].
- [4] D. E. Kharzeev, L. D. McLerran, and H. J. Warringa, The Effects of topological charge change in heavy ion collisions: 'Event by event P and CP violation', *Nucl.Phys.* **A803**, 227 (2008), arXiv:0711.0950 [hep-ph].
- [5] B. Abelev *et al.* (STAR Collaboration), Azimuthal Charged-Particle Correlations and Possible Local Strong Parity Violation, *Phys.Rev.Lett.* **103**, 251601 (2009), arXiv:0909.1739 [nucl-ex].
- [6] B. Abelev *et al.* (STAR Collaboration), Observation of charge-dependent azimuthal correlations and possible local strong parity violation in heavy ion collisions, *Phys.Rev.* **C81**, 054908 (2010), arXiv:0909.1717 [nucl-ex].
- [7] L. Adamczyk *et al.* (STAR), Beam-energy dependence of charge separation along the magnetic field in Au+Au collisions at RHIC, *Phys. Rev. Lett.* **113**, 052302 (2014), arXiv:1404.1433 [nucl-ex].
- [8] L. Adamczyk *et al.* (STAR), Fluctuations of charge separation perpendicular to the event plane and local parity violation in $\sqrt{s_{NN}} = 200$ GeV Au+Au collisions at the BNL Relativistic Heavy Ion Collider, *Phys. Rev.* **C88**, 064911 (2013), arXiv:1302.3802 [nucl-ex].
- [9] J. Zhao (STAR), Chiral magnetic effect search in p+Au, d+Au and Au+Au collisions at RHIC, *Proceedings, 47th International Symposium on Multiparticle Dynamics (ISMD2017): Tlaxcala, Tlaxcala, Mexico, September 11-15, 2017*, EPJ Web Conf. **172**, 01005 (2018), arXiv:1712.00394 [hep-ex].
- [10] J. Zhao (STAR), Charge dependent particle correlations motivated by chiral magnetic effect and chiral vortical effect, *Proceedings, 46th International Symposium on Multiparticle Dynamics (ISMD 2016): Jeju Island, South Korea, August 29-September 2, 2016*, EPJ Web Conf. **141**, 01010 (2017).
- [11] J. Zhao, Measurements of the chiral magnetic effect with background isolation in 200 gev au+au collisions at star, *Nuclear Physics A* **982**, 535 (2019), the 27th International Conference on Ultrarelativistic Nucleus-Nucleus Collisions: Quark Matter 2018.
- [12] L. Adamczyk *et al.* (STAR), Measurement of charge multiplicity asymmetry correlations in high-energy nucleus-nucleus collisions at $\sqrt{s_{NN}} = 200$ GeV, *Phys. Rev.* **C89**, 044908 (2014), arXiv:1303.0901 [nucl-ex].
- [13] V. Khachatryan *et al.* (CMS), Observation of charge-dependent azimuthal correlations in p-Pb collisions and its implication for the search for the chiral magnetic effect, *Phys. Rev. Lett.* **118**, 122301 (2017), arXiv:1610.00263 [nucl-ex].
- [14] B. Abelev *et al.* (ALICE), Charge separation relative to the reaction plane in Pb-Pb collisions at $\sqrt{s_{NN}} = 2.76$ TeV, *Phys.Rev.Lett.* **110**, 012301 (2013), arXiv:1207.0900 [nucl-ex].
- [15] S. Acharya *et al.* (ALICE), Constraining the magnitude of the Chiral Magnetic Effect with Event Shape Engineering in Pb-Pb collisions at $\sqrt{s_{NN}} = 2.76$ TeV, *Phys. Lett.* **B777**, 151 (2018), arXiv:1709.04723 [nucl-ex].
- [16] A. M. Sirunyan *et al.* (CMS Collaboration), Constraints on the chiral magnetic effect using charge-dependent azimuthal correlations in p-pb and pb-pb collisions at the cern large hadron collider, *Phys. Rev. C* **97**, 044912 (2018).
- [17] S. A. Voloshin, Parity violation in hot QCD: How to detect it, *Phys.Rev.* **C70**, 057901 (2004), arXiv:hep-ph/0406311 [hep-ph].
- [18] F. Wang, Effects of Cluster Particle Correlations on Local Parity Violation Observables, *Phys.Rev.* **C81**, 064902 (2010), arXiv:0911.1482 [nucl-ex].
- [19] A. Bzdak, V. Koch, and J. Liao, Remarks on possible local parity violation in heavy ion collisions, *Phys.Rev.* **C81**, 031901 (2010), arXiv:0912.5050 [nucl-th].
- [20] S. Schlichting and S. Pratt, Charge conservation at energies available at the BNL Relativistic Heavy Ion Collider and contributions to local parity violation observables, *Phys.Rev.* **C83**, 014913 (2011), arXiv:1009.4283 [nucl-th].
- [21] H.-j. Xu, X. Wang, H. Li, J. Zhao, Z.-W. Lin, C. Shen, and F. Wang, Importance of isobar density distributions on the chiral magnetic effect search, *Phys. Rev. Lett.* **121**, 022301 (2018).

- [22] H.-J. Xu, J. Zhao, X.-B. Wang, H.-L. Li, Z.-W. Lin, C.-W. Shen, and F.-Q. Wang, Varying the chiral magnetic effect relative to flow in a single nucleus-nucleus collision, *Chinese Physics C* **42**, 084103 (2018).
- [23] J. Liao, V. Koch, and A. Bzdak, On the Charge Separation Effect in Relativistic Heavy Ion Collisions, *Phys.Rev.* **C82**, 054902 (2010), arXiv:1005.5380 [nucl-th].
- [24] A. Bzdak, V. Koch, and J. Liao, Azimuthal correlations from transverse momentum conservation and possible local parity violation, *Phys.Rev.* **C83**, 014905 (2011), arXiv:1008.4919 [nucl-th].
- [25] S. Pratt, S. Schlichting, and S. Gavin, Effects of Momentum Conservation and Flow on Angular Correlations at RHIC, *Phys.Rev.* **C84**, 024909 (2011), arXiv:1011.6053 [nucl-th].
- [26] H. Petersen, T. Renk, and S. A. Bass, Medium-modified Jets and Initial State Fluctuations as Sources of Charge Correlations Measured at RHIC, *Phys.Rev.* **C83**, 014916 (2011), arXiv:1008.3846 [nucl-th].
- [27] V. Toneev, V. Konchakovski, V. Voronyuk, E. Bratkovskaya, and W. Cassing, Event-by-event background in estimates of the chiral magnetic effect, *Phys.Rev.* **C86**, 064907 (2012), arXiv:1208.2519 [nucl-th].
- [28] J. Zhao, Search for the Chiral Magnetic Effect in Relativistic Heavy-Ion Collisions, *Int. J. Mod. Phys.* **A33**, 1830010 (2018), arXiv:1805.02814 [nucl-ex].
- [29] F. W. Jie Zhao, Zhoudunming Tu, Status of the chiral magnetic effect search in relativistic heavy-ion collisions, *Nuclear Physics Review* **35**, 225 (2018), arXiv:1807.05083 [nucl-ex].
- [30] J. Zhao and F. Wang, Experimental searches for the chiral magnetic effect in heavy-ion collisions, *Prog. Part. Nucl. Phys.* **107**, 200 (2019), arXiv:1906.11413 [nucl-ex].
- [31] F. Wang and J. Zhao, Challenges in flow background removal in search for the chiral magnetic effect, *Phys. Rev.* **C95**, 051901 (2017), arXiv:1608.06610 [nucl-th].
- [32] Y. Feng, J. Zhao, and F. Wang, Responses of the chiral-magnetic-effect-sensitive sine observable to resonance backgrounds in heavy-ion collisions, *Phys. Rev. C* **98**, 034904 (2018), arXiv:1803.02860 [nucl-th].
- [33] J. Adams *et al.* (STAR), Rho0 production and possible modification in Au+Au and p+p collisions at $S(NN)^{1/2} = 200$ -GeV, *Phys. Rev. Lett.* **92**, 092301 (2004), arXiv:nucl-ex/0307023 [nucl-ex].
- [34] S. Adler *et al.* (PHENIX Collaboration), Suppressed π^0 production at large transverse momentum in central Au+Au collisions at $S(NN)^{1/2} = 200$ GeV, *Phys.Rev.Lett.* **91**, 072301 (2003), arXiv:nucl-ex/0304022 [nucl-ex].
- [35] J. Adams *et al.* (STAR), Identified particle distributions in pp and Au+Au collisions at $s(NN)^{1/2} = 200$ GeV, *Phys. Rev. Lett.* **92**, 112301 (2004), arXiv:nucl-ex/0310004 [nucl-ex].
- [36] B. Abelev *et al.* (STAR Collaboration), Systematic measurements of identified particle spectra in *pp*, *d*+Au and Au+Au collisions from STAR, *Phys.Rev.* **C79**, 034909 (2009), arXiv:0808.2041 [nucl-ex].
- [37] J. Adams *et al.* (STAR Collaboration), Azimuthal anisotropy in Au+Au collisions at $s(NN)^{1/2} = 200$ -GeV, *Phys.Rev.* **C72**, 014904 (2005), arXiv:nucl-ex/0409033 [nucl-ex].
- [38] A. Adare *et al.* (PHENIX), Azimuthal anisotropy of neutral pion production in Au+Au collisions at $\sqrt{s_{NN}} = 200$ GeV: Path-length dependence of jet quenching and the role of initial geometry, *Phys. Rev. Lett.* **105**, 142301 (2010), arXiv:1006.3740 [nucl-ex].
- [39] X. Dong, S. Esumi, P. Sorensen, N. Xu, and Z. Xu, Resonance decay effects on anisotropy parameters, *Phys. Lett.* **B597**, 328 (2004), arXiv:nucl-th/0403030 [nucl-th].
- [40] L. Adamczyk *et al.* (STAR), Measurements of Dielectron Production in Au+Au Collisions at $\sqrt{s_{NN}} = 200$ GeV from the STAR Experiment, *Phys. Rev.* **C92**, 024912 (2015), arXiv:1504.01317 [hep-ex].
- [41] K. A. Olive *et al.* (Particle Data Group), Review of Particle Physics, *Chin. Phys.* **C38**, 090001 (2014).
- [42] B. Abelev *et al.* (STAR Collaboration), Studying Parton Energy Loss in Heavy-Ion Collisions via Direct-Photon and Charged-Particle Azimuthal Correlations, *Phys.Rev.* **C82**, 034909 (2010), arXiv:0912.1871 [nucl-ex].